JOURNAL OF MATERIALS SCIENCE 21 (1986) 679–686

Varistor–capacitor characteristics of ZnO ceramics

P. Q. MANTAS, A. M. R. SENOS, J. L. BAPTISTA
Departamento de Engenharia Cerâmica e do Vidro e Centro de Cerâmica e Vidro (INIC), Universidade de Aveiro, 3800 Aveiro, Portugal

Electrical properties of ZnO ceramics quenched from several temperatures during the cooling down from sintering temperature were correlated with microstructural changes. Barrier parameters were determined and their variation was interpreted under the assumption that measured donor densities were due to extrinsic donor defects segregated at grain boundaries. A dependence between the concentration gradient of the segregated species and the degradation behaviour of the samples is proposed and correlates well with the experimental data.

1. Introduction

ZnO varistors are non-ohmic devices used as voltage supressors in a large variety of power systems and electronic circuits [1]. These devices are multiphase ceramics made from ZnO and several additives, sintered at temperatures typically above 1200° C and cooled at slow rates to room temperature. A liquid phase is present at sintering temperatures and, upon cooling, several phases have been identified in the varistors [2–4]. The non-ohmic behaviour has, however, been attributed to a thin layer containing additives segregated at the grain boundaries of the ZnO grains [5–7].

The useful characteristics of these devices are altered after some time under electrical bias. This degradation phenomenon manifests itself mainly by alterations in the pre-breakdown and onset of the breakdown regions of the current–voltage varistor curve [7–9]. It is therefore important to understand what influences varistor conduction in these regions.

In this paper we present experimental data on electrical parameters and microstructure of varistor samples sintered at high temperatures and slowly cooled to room temperature, and of samples quenched from various temperatures during the cooling period. These samples had different electrical characteristics, and some of them were used to study degradation behaviour under d.c. fields. It has been shown that although the barrier height increases during the cooling-down period from the sintering temperature, the variations in donor density and in surface electron trap density do not follow the same trend [10].

2. Experimental procedure

Samples of ZnO with the additives Sb_2O_3, Bi_2O_3, Co_2O_3, Cr_2O_3 and MnO_2 were prepared by milling and calcining mixtures of the oxide powders. Two batches of samples were prepared with the listed additives in the molar ratios 2:1:1:1:1. In the first batch the molar ratio of ZnO to additives was 97:3 and in the second batch this ratio was 91:9.

After calcination, the dried powder was pressed into disks of 2 cm diameter and 1.5 to 2 mm height and sintered at 1350° C for 1 h. The rate of cooling from the sintering temperature was controlled at 1° C min^{-1}. Some samples were quenched from selected temperatures during the cooling period. Before quenching they were maintained for 2 h at that temperature. After lapping, circular gold electrodes were sputtered on to opposite sides of the samples.

The current–voltage characteristics were measured using d.c. current up to about 2 mA and using voltage pulses for higher currents. Resistivity measurements were obtained up to 140 to 160° C, in the ohmic region of the samples. Capacitance measurements were made at room temperature at a constant frequency of 1.585 kHz.

Degradation of selected samples was conducted under d.c. bias, at constant stabilized current, at 150° C. When the degradation run was completed, the samples were quickly cooled to temperatures below room temperature by immersion in liquid nitrogen. The applied d.c. field was then turned off and, after the samples had warmed up to room temperature, V–I and C–V characteristics were measured as described previously.

Conventional techniques were used for scanning electron microscopic (SEM) observation of the samples.

3. Results and discussion

3.1. V–I and C–V curves

The V–I curves measured at room temperature, for samples containing 3 mol % of additives, quenched from various temperatures as well as slowly cooled, are presented in Fig. 1. The resistivity of the samples increased when the quenching temperature decreased, with progressive improvement of the non-ohmic characteristics. The trend was the same but less pronounced for samples with the higher additive content of 9 mol %.

Fig. 2 shows the capacitance dependence on the d.c. voltage bias for the same samples as in Fig. 1. With the exception of the samples quenched from the

0022–2461/86 $03.00 + .12

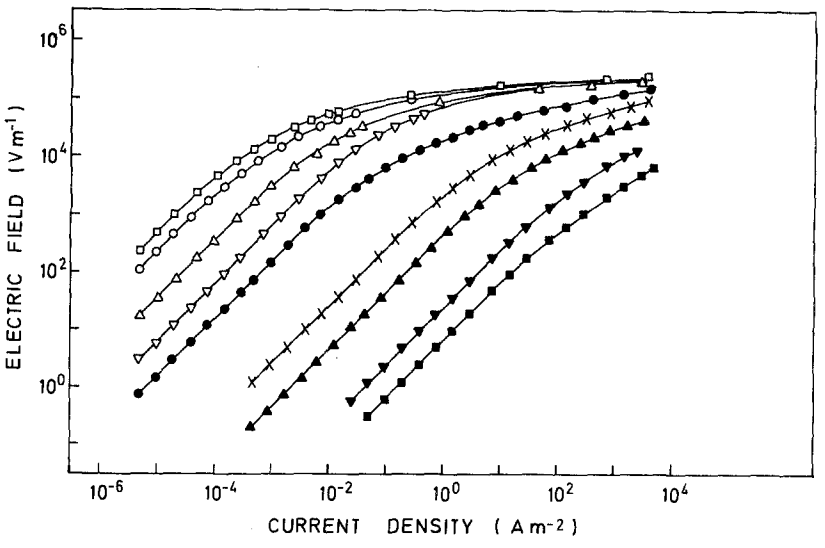

Figure 1 V–I characteristics of quenched samples: (○) room temperature, (□) 665° C, (△) 757° C, (▽) 842° C, (●) 950° C, (x) 1042° C, (▲) 1150° C, (▼) 1250° C, (■) 1350° C.

temperature at which sintering was conducted (1350° C), whose capacitance did not vary with the applied voltage, it can be seen that increasing the d.c. field caused first a decrease and later an increase in the measured capacitance. This last behaviour, of increasing capacitance with applied voltage, occurs at lower d.c. voltages for samples quenched from higher temperatures. Also the zero bias capacitance is higher for samples quenched from higher temperatures, the variation being most marked at temperatures above 842° C.

SEM observations of both sets of samples, using backscattered electrons, showed that the phases previously identified in ZnO varistors [2–4] were present at all temperatures. Using the attachment for energy-dispersive X-ray analysis (EDAX) we identified the constituents of each phase without attempting quantitative analysis. For simplicity, we will call the zinc-rich phase ZnO, the antimony-rich phase spinel, and the bismuth-rich phase the bismuth phase, without regard for the exact compositions.

The bismuth phase in samples quenched from the higher temperature had the appearance of a liquid spreading over large areas of ZnO and spinel grains. Upon lowering the quenching temperature it could be seen that a large portion of this phase had disappeared by 1200° C and that there was a tendency for it to be found mainly in spinel–spinel and spinel–ZnO grain contacts and not in ZnO–ZnO grain contacts. Fig. 3 shows the microstructures of samples containing 9% of additives, quenched from the sintering temperature and from lower temperatures, as well as that of a sample slowly cooled to room temperature. No new

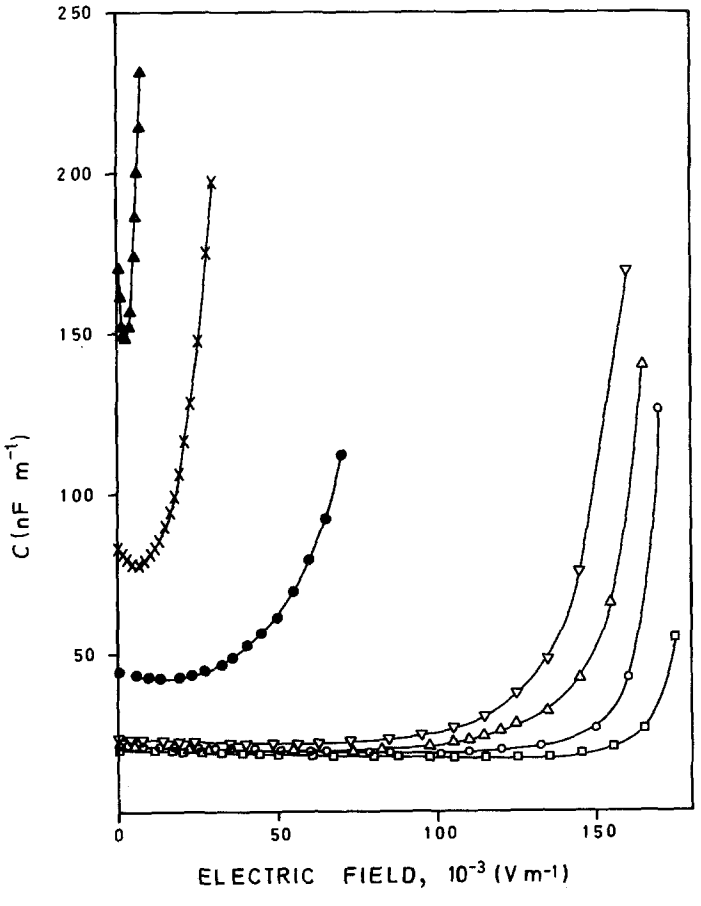

Figure 2 Dependence of capacitance on the applied d.c. field: (○) room temperature, (□) 665° C, (△) 757° C, (▽) 842° C, (●) 950° C, (x) 1042° C, (▲) 1150° C.

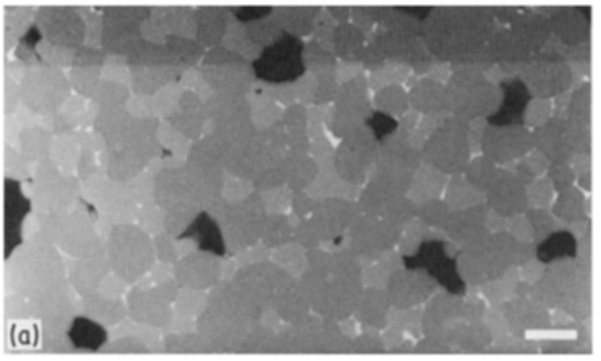

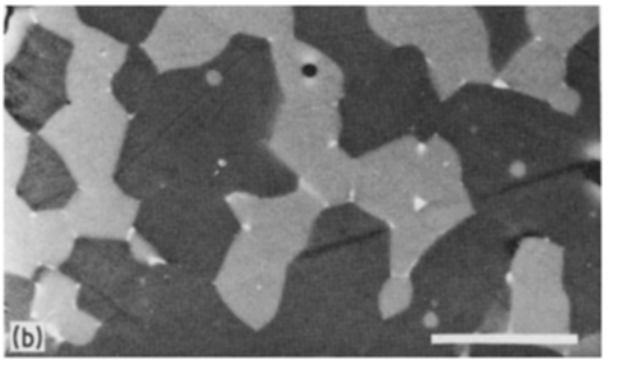

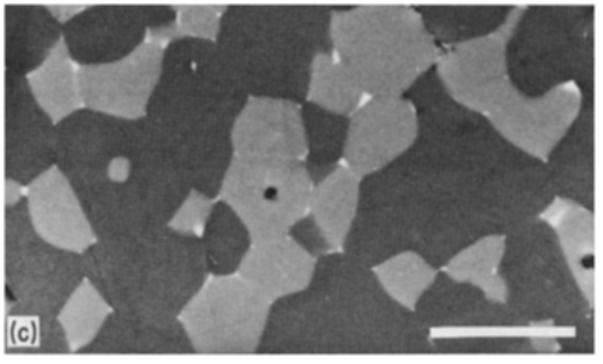

Figure 3 SEM micrographs (a) quenching from 1350° C, (b) quenching from 1250° C, (c) slowly cooled to room temperature (bar = 10 μm).

phases could be seen in the samples with the high additive content, as reported previously [11], and the higher proportion of additives produced the microstructural changes. The relative proportion of the spinel phase was small, however, in samples containing 3% of additives.

The variations in the V–I curves can be explained in part by taking into consideration the observed changes in the microstructures of the samples. Increasingly non-ohmic behaviour was observed to occur below 1200° C, after the majority of the bismuth-rich phase had disappeared. The disappearance of the liquid phase would be accompanied by the precipitation of ZnO and spinel, with some additives in solid solution. The microstructures observed indicate that the liquid tended to remain mainly between spinel–spinel and spinel–ZnO grains, and in doing so, ZnO–ZnO contacts will be formed, i.e. the grain boundaries usually associated with non-ohmic behaviour. The increase in non-ohmic characteristics observed after this, as cooling down continues, would seem therefore to be caused by changes in the structure of these ZnO–ZnO grain boundaries already free from the extra bismuth-rich phase.

The exact origin of the high capacitance values measured at zero bias for samples quenched from high temperatures, as shown in Fig. 2, is not fully understood. Contributions from a bismuth-rich phase to the capacitance of commercial low-voltage varistors have been reported [12]. Differences in resistance among grain boundaries in polycrystalline varistors have also been indicated as a possible cause for the observed frequency dependence of zero bias capacitance [13].

Our samples showed variations with temperatures of the contact area between the solid grains and the bismuth-rich phase, which was liquid at quenching temperature. Variations with temperature in the composition of the liquid phase in the composition of the grain boundaries would be expected. The variations might cause the observed changes in zero-bias capacitance for the samples quenched from temperatures above 842° C.

The variation of capacitance as a function of the applied field, however, seems to be associated with ZnO–ZnO contacts free from the bismuth-rich phase, since there was no variation of capacitance with the bias field for samples quenched from the sintering temperature, i.e. where large areas of bismuth-rich phase could be seen contacting the grains. If this is so, these variations could then be used to investigate the nature of the ZnO–ZnO grain boundaries for the various samples.

3.2. Schottky barrier parameters

Using the measured capacitance values from Fig. 2, we plotted the function $(1/C - 1/2C_0)^2$ against V in Fig. 4. Assuming that the region of good linearity was representative of the capacitance of double Schottky barriers at ZnO grain boundaries, we calculated the donor density, N_D, in each case from the slopes of the straight lines, using the equation [14]

$$\left(\frac{1}{C} - \frac{1}{2C_0}\right)^2 = \frac{2\,(E_B + qV)}{q^2 \varepsilon \varepsilon_0 N_D} \qquad (1)$$

where C and C_0 are capacitance per grain boundary at voltage V and zero voltage respectively, ε is the permittivity of ZnO (8.5), ε_0 the permittivity of free space, q the electronic charge and E_B the barrier height, identified here with the activation energy for charge transport in the low-field ohmic region of the varistor V–I curves. E_B was obtained from the slopes of the resistivity against reciprocal temperatures plots shown in Fig. 5. Small variations in barrier height in the temperature range used for measurements of resistivity were ignored [15].

Having determined the donor density and the height of the Schottky barrier, the density of electron trap states in the grain boundary, N_T, was calculated for all quenched samples taking into consideration the known dependence of the barrier height on N_T^2/N_D [15, 16], using equation [17]

$$E_B = \frac{q^2 N_T^2}{2\,\varepsilon \varepsilon_0 N_D} \qquad (2)$$

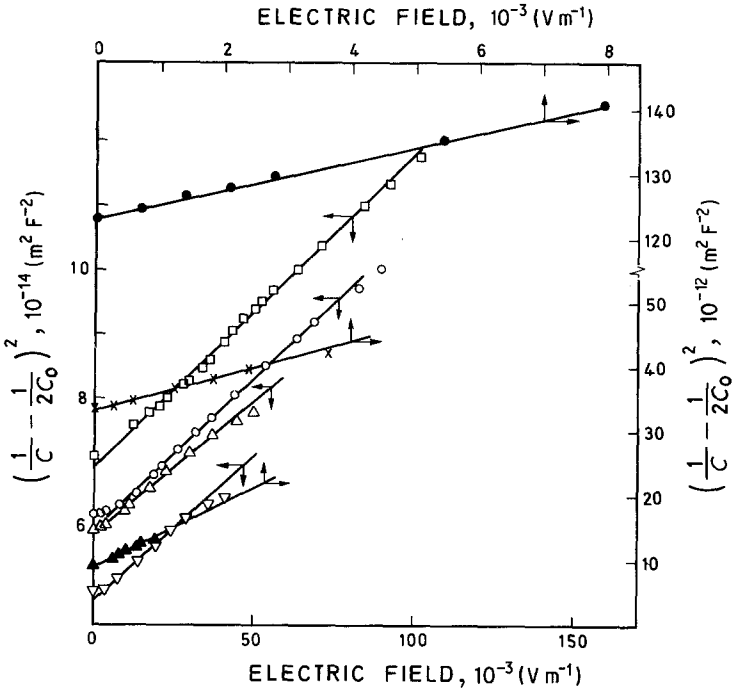

Figure 4 Dependence of $(1/C - 1/2C_0)^2$ on the applied d.c. field: (○) room temperature, (□) 665° C, (△) 757° C, (▽) 842° C, (●) 950° C, (×) 1042° C, (▲) 1150° C.

This simple relation between the parameters was used because the structure of the grain-boundary region is not known in sufficient detail to warrant the use of more specific models. N_T is therefore the total density of electron traps, undifferentiated with respect to their energy levels.

The calculated values of E_B, N_D and N_T are plotted in Fig. 6 against the temperatures of quenching. If one ignores the time that each sample was maintained at the temperature from which it was quenched (2 h), the abcissa could be considered equally well as a time scale, since the cooling rate was constant at 1° C min^{-1}.

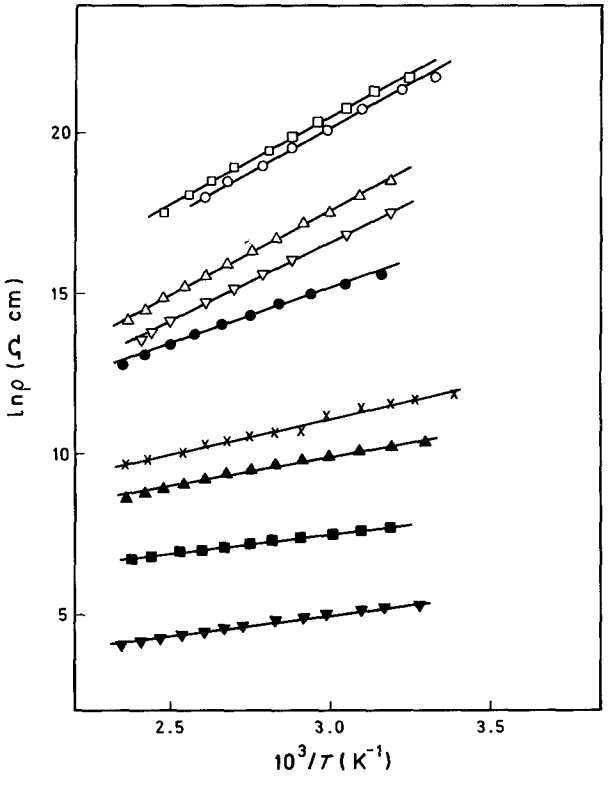

Figure 5 Resistivity against temperature: (○) room temperature, (□) 665° C, (△) 757° C, (▽) 842° C, (●) 950° C, (×) 1042° C, (▲) 1150° C, (■) 1250° C, (▼) 1350° C.

In this figure one can follow the rise of the electrical barrier as the samples are cooled from the sintering temperature to room temperature. The barrier grows starting from about 1200° C down to about 600° C, where it levels off at the values measured for samples slowly cooled to room temperature. Two distinct growth rates can be observed.

When consideration is taken of the observed changes in the density of donors in the depletion layers and of the density of electron traps in the boundary surface, it can be seen that although both concentrations were increasing during the initial stages of the growth of the electrical barrier, they decreased during the final stage. At 842° C, where the barrier height was almost at its maximum value, both concentrations had lower values than their maxima, which were attained at a temperature near 950° C corresponding to the inflection point in the barrier-height curve.

The defect chemistry of ZnO varistors is not known in any detail, the role played by intrinsic and extrinsic defects in the observed properties of these devices being uncertain. There is also still controversy on the nature of intrinsic donor defects in pure ZnO, the alternatives being the oxygen vacancy [18–20] or the zinc interstitial defect [21–23]. It is, however, difficult to understand how the donor concentrations calculated from the capacitance measurements could correspond to intrinsic defect concentrations, particularly at the higher temperatures, since the equilibrium concentration of defects should decrease with temperature [20, 27] and not increase as observed in Fig. 6. On the other hand, there is experimental evidence which shows that added impurities control the concentration of donors present in ZnO varistors [24] and that varistors sintered at different O_2 pressures showed no alteration in the density of donors present in the bulk of ZnO grains, but did have different concentrations of surface traps [25].

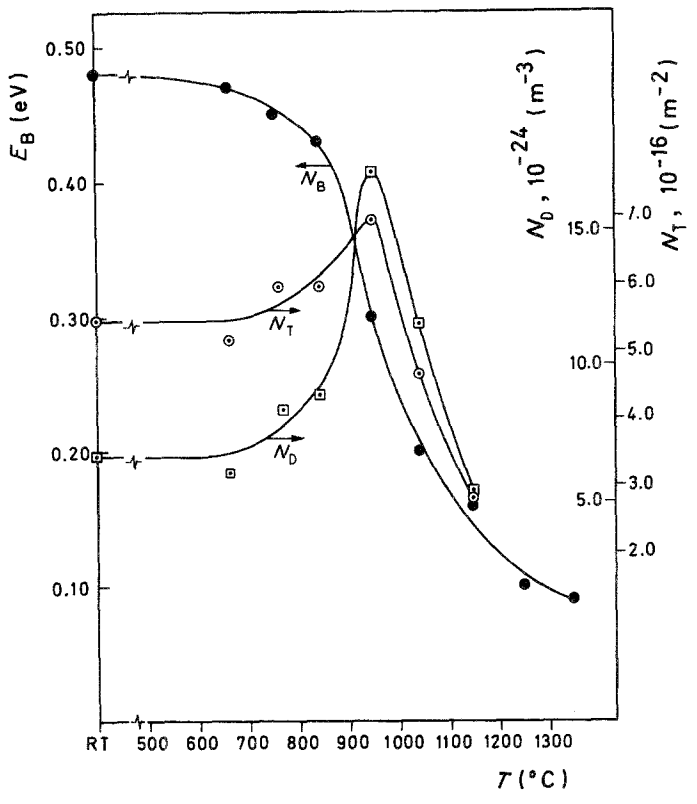

Figure 6 Variation of E_B, N_D and N_T with temperature (RT = room temperature).

It is therefore more likely that defects due to soluble additives are the ones responsible for the rise in the donor density and in the electron trap density. The variations observed in donor concentration in the high-temperature region are probably evidence for an increasing concentration of donor dopants in the grain-boundary region. As a result of the precipitation of ZnO from the bismuth-rich phase, and of structural differences between the grain boundary and the bulk of ZnO grains, segregation towards the grain-boundary region would take place during cooling. The increase in barrier height during this stage could come therefore as a result of the increase in concentration of dopants in the grain-boundary region.

The values for the donor concentration and surface state concentration obtained here rely on the model of a Schottky barrier being formed on each side of the ZnO grain boundary. A different approach for the mechanism of electrical barrier formation has been proposed by Einzinger [26, 27], who argued that the barriers present in polycrystalline ZnO varistors could be the result of non-equilibrium conditions generated during the cooling period. The concentration of vacancies or interstitial defects present at higher temperatures would not attain the equilibrium values characteristic of low temperatures, due to the decrease in diffusivities of those defects at low temperatures. In this way, only the surface of the ZnO grains would have the equilibrium concentration values, the concentration in the bulk being higher. The low concentration of intrinsic donor defects near the surface, causing a low concentration of electrons there, would lower the position of the Fermi level, and for Fermi level equilibrium the conduction band would rise near the surface, giving a potential barrier for electrons.

Mahan [20] calculated that the expected rise in barrier height by this mechanism would not exceed 0.1 eV, and concluded that it could not be the main source of barrier formation in ZnO varistors.

Our experimental results on the high-temperature side of Fig. 6 seem to support Mahan's conclusion. However, the small increase in barrier height observed below 842° C could well have resulted from the mechanism proposed by Einzinger, since it should be particularly operative at the lowest temperatures, where thermodynamic equilibrium would be more difficult to achieve. The low values for the donor concentration would then be equilibrium values for the intrinsic defect concentration near the surface, the bulk values being still higher than those measured in the depletion layers. This would mean that in this temperature region our samples did not come to equilibrium even after 2 h of annealing at the temperature from which they were quenched. To test this hypothesis we subjected one sample to an annealing time of 60 h at 650° C before quenching. The results do not support this interpretation, since we did not detect significant variations in barrier height or in donor density. Either the diffusivity at this temperature is so small as to make the differences not detected, or even in this low-temperature region the mechanism is different, the barrier still rising due to different variations in the concentration of N_D and N_T, the latter being most likely controlled by the atmosphere composition [25]. If the values measured for the density of donors resulted from extrinsic defects segregating at the boundaries, either exsolution due to saturation or defect cluster formation could cause the observed decrease in donor concentration in the low temperature region. We have no experimental evidence for either effect.

3.3. Degradation

The samples quenched from 842, 757 and 665° C and the ones slowly cooled to room temperature, which

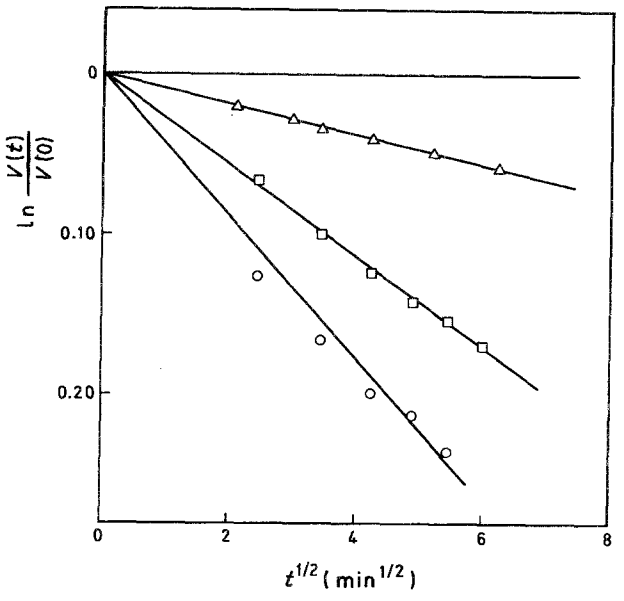

Figure 7 $\ln V(t)/V(0)$ against $t^{1/2}$: (○) room temperature, (□) 665° C, (△) 757° C, (—) 842° C.

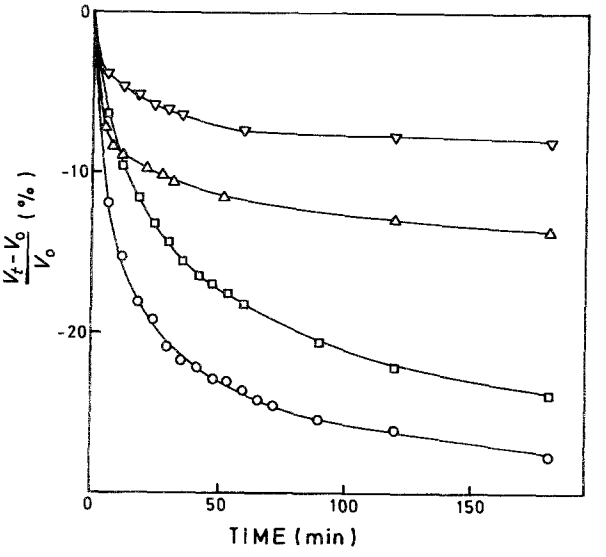

Figure 8 Degradation as a function of time: (○) room temperature, (□) 665° C, (△) 757° C, (▽) 842° C.

showed the most non-ohmic characteristics and presented the smallest differences in barrier heights, were subjected to degradation at 150° C under constant d.c. currents.

In one set of samples the same d.c. current density of 0.250 mA cm^{-2} was applied to each sample during the degradation period. Under these conditions only the samples cooled slowly to room temperature and those quenched from 665 and 757° C degraded. No degradation was observed for the samples quenched from 842° C even after 25 h under the applied field. In Fig. 7 we have plotted $\ln V(t)/V(0)$ against $t^{1/2}$, where $V(0)$ is the initial value of field strength and $V(t)$ the field value after time t has elapsed. A straight-line relation is obtained in every case, a result that is consistent with a diffusion process taking place under the action of the applied field. Several authors have concluded that degradation in ZnO varistors is associated with ion migration under the influence of the applied field [8, 9, 28]. Accumulation of cations at grain boundaries in degraded varistors has also been observed [7].

Assuming an empirical relation of the form

$$V(t) = V(0) \exp(-Kt^{\frac{1}{2}}) \quad (3)$$

with $K = (1/\tau)^{1/2}$, we calculated the τ values presented in Table I, τ being a time constant related to the degradation behaviour of each sample. It can be concluded that under these experimental conditions the stability against degradation decreased as the quenching temperature of the samples decreased.

For another set of samples, a constant current was chosen such that every sample was subjected to the same initial field strength, namely, 450 V cm^{-1}. In Fig. 8 we present the percentage variation in field strength during a 3 h degradation period. A rapid initial decrease in field was observed for every sample, followed by a much slower variation. Again we can conclude from this experiment that samples degraded to a higher extent as the quenching temperature decreased. Fig. 9 shows the V–I curves of one sample quenched from 665° C, before and after a degradation period of 3 h. Different symbols indicate measurements with the field applied in the same direction and in the reverse direction, respectively, relative to the direction of the degradation field. A decrease in barrier height could be inferred from this figure.

TABLE I Time constants (min) for degradation under constant current density

ζ_{RT}*	$= 7.0 \times 10^2$
ζ_{665}	$= 1.4 \times 10^3$
ζ_{757}	$= 1.1 \times 10^4$
ζ_{842}	$= \infty$

*RT = room temperature

Alteration in barrier parameters under the applied field seems to be the cause of degradation of ZnO varistors [8, 28]. The decrease in barrier height, associated with degradation, could take place either due to an increase in concentration of donors in the depletion region or to a decrease in the concentration of electron surface states at the grain boundaries. Gupta and Carlson [9] suggested that diffusion of interstitial zinc ions ($Zn_i^{\cdot}$) in the depletion layer would take place under the action of the applied field, and that they would combine with negative species at the boundary to form neutral species. This simultaneous decrease in donor and acceptor species could also result in a decrease of the barrier height.

Our results indicate that the less degradable samples were those quenched from higher temperatures. The trends observed in Fig. 6 for the variation in barrier parameters of samples that were later subjected to degradation suggest some sort of correlation between the donor concentration values measured before degradation and the degradation behaviour of the various samples, since the concentration of acceptor states at the boundaries showed little variation during the cooling period.

Assuming that degradation of ZnO varistors is diffusion-dependent, as experimental results suggest, one could envisage their degradation as the result of the accumulation of positively charged species driven

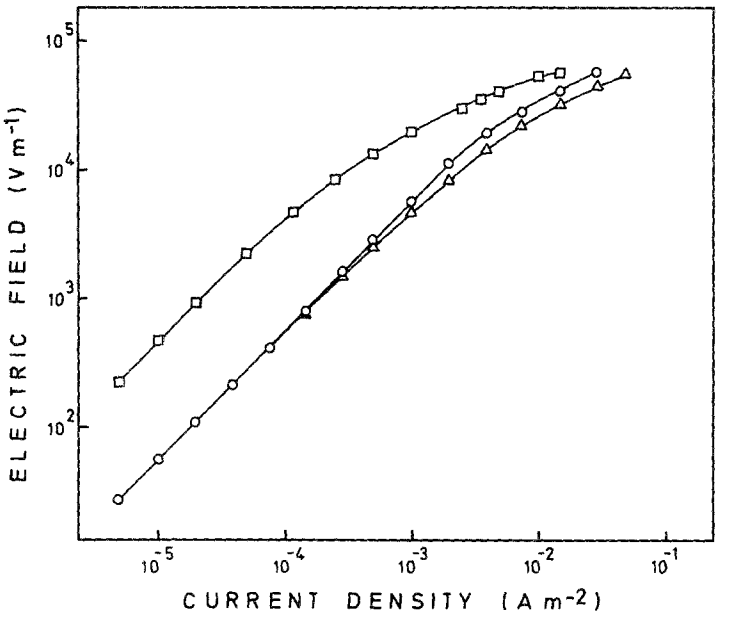

Figure 9 V–I characteristics of samples quenched from 665° C (□) before and (○, △) after degradation; (○) field direction same as that of degradation field, (△) reverse direction.

by the applied field towards the boundary region. These donor species may or may not react with the acceptor species present at the grain boundary. The movement of the charged species will be opposed by any concentration gradient of the same species, whether pre-existing or originating from the build-up in the grain-boundary region. Degradation will slow down as the chemical concentration gradient increases, and will stop when equilibrium between the applied electrical potential and the chemical potential is reached. According to this mechanism, the higher the slope of the concentration profile of the segregated donor species in the boundary region, the less degradable a varistor would be.

The donor concentration was observed to decrease below 950° C, as seen from Fig. 6, probably due to exsolution at the grain boundary or the formation of defect clusters near the boundary where segregation was more severe. The resultant decrease in the concentration gradient near the boundary decreases the chemical potential opposing donor migration due to the influence of the applied electric field. It would therefore be expected that the tendency for degradation would be greater if the varistor were cooled slowly through this temperature region. Our results are in qualitative agreement with this prediction, since the varistors with higher donor concentrations were those that degraded to a lesser extent.

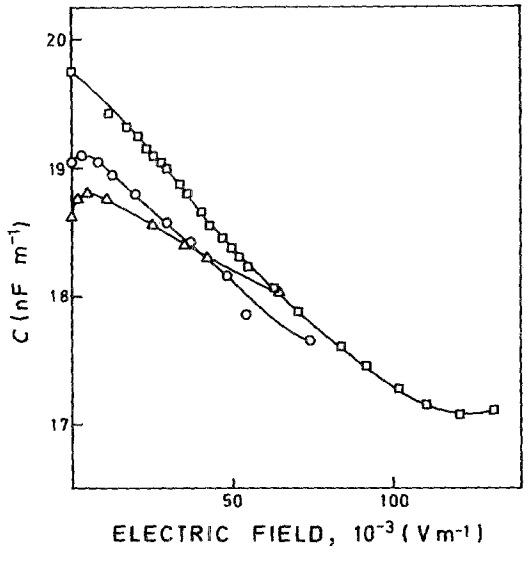

Figure 10 Dependence of capacitance on the applied d.c. voltage of sample quenched from 665° C (□) before and (○, △) after degradation; (○) field direction same as that of degradation field, (△) reverse direction.

If this is the mechanism responsible for varistor degradation one would also expect some quantitative correlation between the changes in donor concentration and the degradation that took place. To check this we measured the C–V characteristics of the degraded samples. Fig. 10 shows the variation of capacitance with the applied field for one of the samples, before and after degradation. The symbols have the same meaning as in Fig. 9. It can be seen that the main variation during degradation took place in the reverse state of the applied field, where migration towards the boundary of the positively charged species would be expected to occur.

Values for the concentration of donors in the reverse state of the applied field were calculated from plots of $(1/C - 1/2C_0)^2$ against V and are presented in Table II, together with the values for non-degraded samples. It can be seen that after degradation each sample attained similar values for the donor density ($1.30 \pm 0.08 \times 10^{25}\,m^{-3}$) as would be expected for the proposed mechanism, since the measured increase in donor concentration would be the result of the accumulation of ionized donors near the boundary,

TABLE II Donor density before and after degradation

Quenching temperature (° C)	N_D (m^{-3}) before degradation	N_D (m^{-3}) after degradation
Room temperature	6.62×10^{24}	1.29×10^{25}
665	5.98×10^{24}	1.17×10^{25}
757	8.37×10^{24}	1.36×10^{25}
842	9.28×10^{24}	1.39×10^{25}

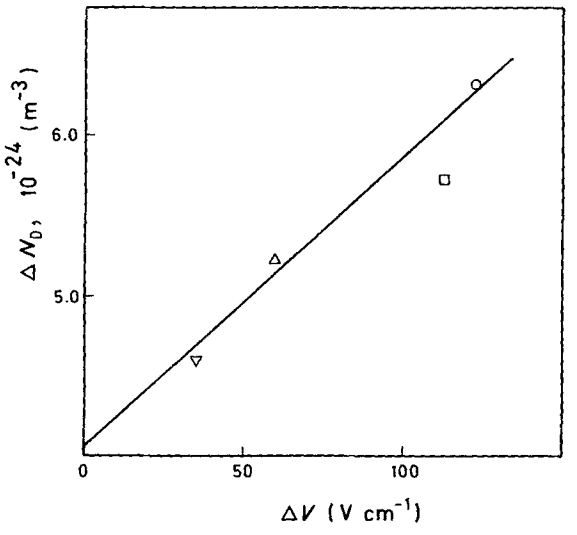

Figure 11 Correlation between degradation and the variation in donor concentration: (○) room temperature, (□) 665° C, (△) 757° C, (▽) 842° C.

with a concomitant increase in the slope of the concentration gradient.

Fig. 11 shows, for the same set of samples, the variation of donor concentration against the amount of degradation, measured by the change in the electrical potential. A reasonable degree of correlation is observed as should be expected.

It is interesting to verify that the straight line in Fig. 11 extrapolates to a value of about $4 \times 10^{24} m^{-3}$ at zero degradation, indicating that degradation would only occur after this change in donor density had taken place. It has been observed in our samples and in samples degraded by other groups [9] that under less severe degradation conditions an induction period exists before degradation starts. Since it is very unlikely that the movement of charged species would not start as soon as the electric field was applied across the grain boundaries, it would seem that the reason why this was not observed under more severe degradation conditions was due to the shorter time necessary for the migration of this quantity of ionized donors. The conclusion that this quantity of ions does not alter the barrier height can be rationalized if the migrated ions affected the surface states in such a way that the balance of the values of N_D and N_T in Equation 2 maintained the barrier height unchanged.

4. Conclusions

1. The $V-I$ and $C-V$ characteristics of varistor samples quenched from various temperatures after slow cooling from the sintering temperature seem to be correlated with concomitant changes in the microstructure.

2. The variations in barrier parameters obtained for the same set of samples are consistent with the interpretation that impurity solute segregation towards the grain boundary region takes place during the cooling process.

3. The degradation characteristics of samples with the best varistor characteristics could be correlated with the concentration of the segregated donor impurities at the grain boundaries.

Acknowledgments

The authors would like to acknowledge the assistance of Eng. Carlos Sá with the SEM. They are also indebted to Professors J. R. Frade and G. P. Wirtz for useful discussions.

References

1. M. MATSUOKA, *Adv. Ceram.* **1** (1981) 129.
2. L. M. LEVINSON and H. R. PHILLIP, *J. Appl. Phys.* **46** (1975) 1332.
3. M. INADA, *Jpn. J. Appl. Phys.* **18** (1979) 8.
4. *Idem, ibid.* **17** (1978) 673.
5. W. G. MORRIS, *J. Vac. Sci. Technol* **13** (1976) 926.
6. D. R. CLARKE, *J. Appl. Phys.* **49** (1978), 2407.
7. YET-MING CHIANG and W. D. KINGERY, *ibid.* **53** (1982) 1765.
8. M. HAYASHI, M. HABA, S. HIRANO, M. OKAMOTO and M. WATANABE, *ibid.* **53** (1982) 5754.
9. T. K. GUPTA and W. G. CARLSON, *ibid.* **53** (1982) 7401.
10. A. M. R. SENOS, P. Q. MANTAS and J. L. BAPTISTA, in Proceedings of Electroceramics Meeting, Brussels, 1984, to be published in Silicates Industriels.
11. M. INADA, *Jpn. J. Appl. Phys.* **17** (1978) 1.
12. R. EINZINGER, *Adv. Ceram.* **1** (1981) 359.
13. G. E. PIKE, *Mater. Res. Soc. Proc.* **5** (1982) 369.
14. K. MUKAE, K. TSUDA and I. NAGASAWA, *J. Appl. Phys.* **50** (1979) 4475.
15. G. E. PIKE and C. H. SEAGER, *Adv. Ceram.* **1** (1981) 53.
16. C. H. SEAGER, *Mater. Res. Soc. Proc.* **5** (1982) 85.
17. W. HEYWANG, *J. Amer. Ceram. Soc.* **47** (1964) 484.
18. E. ZIEGLER, A. HEINRICH, H. OPPERMAN and G. STROVER, *Phys. Status Solidi (A)* **66** (1981) 635.
19. B. SCHALLEMBERGER and A. HAUSMANN, *Z. Phys. B* **44** (1981) 143.
20. G. D. MAHAN, *J. Appl. Phys.* **54** (1983) 3285.
21. J. W. HOFFMAN and I. LAUDER, *Trans. Faraday Soc.* **66** (1970) p. 2346.
22. K. I. HAGEMARK, *J. Solid State Chem.* **16** (1976) 293.
23. G. NEUMANN, *Phys. Status Solidi (B)* **105** (1981) 605.
24. T. MIYOSHI, K. MAEDA, K. TAKAHASHI and T. YAMAZAKI, *Adv. Ceram.* **1** (1981) 309.
25. A. M. R. SENOS and J. L. BAPTISTA, *J. Mater. Sci. Lett.* **3** (1984) 213.
26. R. EINZINGER, *Appl. Phys. Surf. Sci.* **1** (1978) 329.
27. *Idem, Mater. Res. Soc. Proc.* **5** (1982) 343.
28. K. EDA, A. IGA and M. MATSUOKA, *J. Appl. Phys.* **51** (1980) 2678.

Received 25 March
and accepted 22 April 1985